Communication

Benefits of Intercritical Annealing in Quenching and Partitioning Steel

X. WANG, L. LIU, R.D. LIU, and M.X. HUANG

Compared to the quenching and partitioning (Q&P) steel produced by full austenization annealing, the Q&P steel produced by the intercritical annealing shows a similar ultimate tensile stress but a larger tensile ductility. This property is attributable to the higher volume fraction and the better mechanical stability of the retained austenite after the intercritical annealing. Moreover, intercritical annealing produces more ferrite and fewer martensite phases in the microstructure, making an additional contribution to a higher work hardening rate and therefore a better tensile ductility.

https://doi.org/10.1007/s11661-018-4559-6

The quenching and partitioning (Q&P) steel was first proposed by Speer and co-workers[1] and has been considered to be a third-generation advanced high strength steel (AHSS) grade for lightweight automotive applications. The original Q&P concept[1] involves a full austenization annealing at a temperature above Ac3 followed by a fast quenching to a temperature between the martensite start (M_s) and finish (M_f) temperatures. The quenching step forms a microstructure consisting of retained austenite grains embedded in the martensite matrix. Finally, a partitioning step at or above the M_s temperature is employed to allow carbon partitioning from the martensite to the retained austenite. The martensite matrix in the Q&P steel can offer high strength, while the retained austenite provides the transformation-induced plasticity (TRIP) effect for improving ductility.[2] Most existing studies on the Q&P steel focus on tailoring the retained austenite in order to improve the mechanical properties.[3] These studies consider that the Q&P steel contains only a martensite matrix with retained austenite. Nevertheless, a high cooling rate from the austenization temperature to the quenching temperature is required to achieve an ideal microstructure consisting of only the martensite matrix and the retained austenite. Such a high cooling rate can be achieved for small samples fabricated in laboratories. However, most existing industrial production lines (continuous annealing lines) in the steel industry cannot realize such a high cooling rate. It has been shown that the Q&P steel produced in the current industrial production line was cooled slowly from the fully austenitization region to the intercritical region. Such slow cooling results in the formation of proeutectoid ferrite, as well as a nonuniform carbon distribution in the retained austenite, leading to the unsatisfactory mechanical properties.[4] Therefore, it has been suggested that a modified process using intercritical annealing instead of full austenization annealing can be employed to produce the Q&P steel.[5] Such a Q&P steel consists of ferrite, martensite, and retained austenite. Intercritical annealing is now widely used in the steel industry to produce Q&P steel with the tensile strength of 1000 MPa. Nevertheless, the difference between the industrially produced Q&P steel fabricated by a full austenization annealing and intercritical annealing has not been fully investigated to date, especially the difference regarding the microstructure, mechanical properties, and deformation mechanisms. The current study aims to investigate the difference in the Q&P steel produced industrially by the full austenization annealing and the intercritical annealing. Both Q&P steels are produced using a slow cooling rate that is comparable to the cooling rate available in the current industrial production lines.

The steel investigated in the current study has the chemical composition of Fe-0.2C-2.0Mn-1.5Si (in wt pct). The Q&P steel samples are produced in the laboratory using a thermal–mechanical simulator (SURFACE TEC, Germany). The Q&P processes are similar to the processes currently employed in the steel industry. The Ac1 and Ac3 temperatures of the investigated steel are determined by dilatometry tests and are observed to be 733 °C and 867 °C, respectively. Therefore, 780 °C and 900 °C are selected as the intercritical and full austenization annealing temperatures, respectively. The samples produced by intercritical annealing and full austenization annealing are referred to as QP-I and QP-A, respectively. The M_s and M_f temperatures of the cold–rolled samples are determined to be 344 °C and 195 °C by the dilatometry test with the quenching rate of 100 °C/s. The Q&P processes for the QP-I and QP-A samples are illustrated in Figure 1(a). It is noted that the only difference between the QP-I and QP-A samples is the annealing temperature (Figure 1(a)). One can observe that the cooling rate from high temperature (780 °C or 900 °C) to 690 °C is slow (5 °C/s), which inevitably leads to the formation of ferrite during the cooling. Such a slow cooling rate is generally expected in the current industrial annealing lines. Tensile samples

X. WANG and R.D. LIU are with the Iron and Steel Research Institute, Ansteel Group, Anshan, China. L. LIU and M.X. HUANG are with the Department of Mechanical Engineering, the University of Hong Kong, Hong Kong, China. Contact e-mail: mxhuang@hku.hk
Manuscript submitted September 16, 2017.
Article published online March 8, 2018

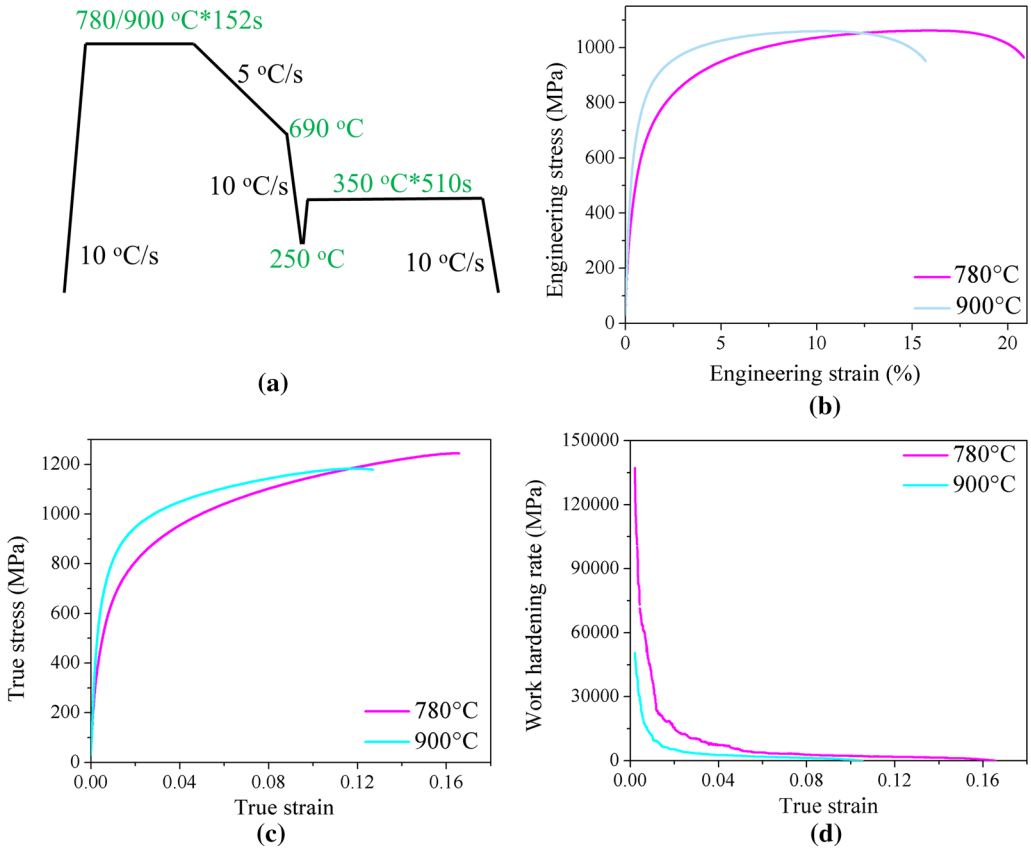

Fig. 1—(*a*) Heat-treatment processes for the QP-I (780 °C) and QP-A (900 °C) samples, (*b*) engineering stress–strain curves, (*c*) true stress–strain curves, and (*d*) work hardening rate of the QP-I (780 °C) and QP-A (900 °C) samples.

with the gauge dimensions of 25 mm in length, 6 mm in width, and 1.4 mm in thickness are prepared along the rolling direction by wire-cut following the ASEM-E8 subsize standard. The tensile tests are performed on a universal testing machine with the quasi-static strain rate of approximately 10^{-3} s^{-1} at room temperature. An extensometer is used for the precise measurements of the strain till fracture. X-ray diffraction (XRD) experiments are performed using a Rigaku diffractometer using Co Kα radiation with the wavelength of 1.79 Å to determine the phase fraction and carbon content of retained austenite. The diffraction peaks, including (2 0 0)α, (2 1 1)α, (2 0 0)γ, (2 2 0)γ, and (3 1 1)γ, are selected for quantitative analysis. The samples for XRD measurements are prepared by electropolishing using a solution mixture of 5 pct perchloric acid and 95 pct acetic acid (vol pct) after conventional mechanical polishing. The microstructure is observed using a Hitachi S4800 scanning electron microscope (SEM).

The engineering stress–strain curves of the QP-I and QP-A samples are shown in Figure 1(b). It can be observed that both samples show similar ultimate tensile strengths (1050 MPa), but the QP-I sample shows a larger uniform and total elongation than the QP-A sample. In other words, the use of intercritical annealing instead of the full austenization can improve the ductility while maintaining the same ultimate tensile strength. Therefore, intercritical annealing is more attractive for automotive applications and is now widely employed by the steel industry for producing the Q&P steel. Figure 1(c) shows the true stress–strain curves until necking for both the QP-I and QP-A samples. The work hardening rates of QP-I and QP-A samples are shown in Figure 1(d). It is shown that the QP-I sample has a higher work hardening rate than the QP-A sample. Therefore, a larger uniform elongation is achieved in the QP-I sample. The microstructures of both QP-I and QP-A samples are shown in Figure 2. Both samples have ferrite, martensite, and retained austenite as shown in Figure 2, differing from the classical Q&P steel consisting of martensite and retained austenite.[6] It is difficult to differentiate the martensite and retained austenite in the SEM images (Figure 2), and they are therefore marked together as martensite/austenite (M/A) in Figure 2.

The volume fraction of retained austenite measured by XRD is shown in Figure 3(a). The area fraction of ferrite and M/A in both the QP-I and QP-A samples are measured using multiple SEM images taken at different locations of the sample. Assuming that the area fraction is approximately the same as the volume fraction, the volume fractions of ferrite, martensite, and retained austenite can therefore be obtained by combining the volume fraction of retained austenite (f_γ) measured by XRD and the area fraction of M/A ($f_{M/A}$) measured by SEM. In other words, the volume fraction of martensite

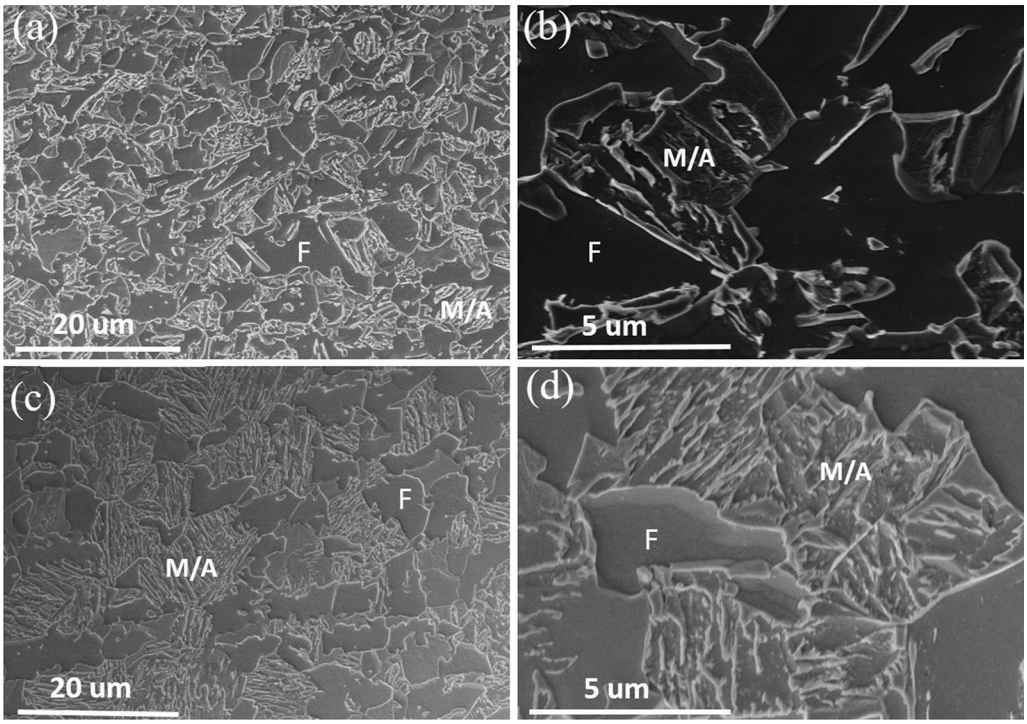

Fig. 2—(*a*), (*b*) microstructure of the QP-I sample; (*c*), (*d*) microstructure of the QP-A sample. *F* represents ferrite, while M/A represents martensite/austenite.

($f_{\alpha'}$) can be obtained as $f_{\alpha'} = f_{M/A} - f_{\gamma}$. Next, the volume fractions of ferrite, martensite, and retained austenite can be obtained. The results are shown in Figure 3(b). As seen from Figure 3(b), the QP-I sample has higher volume fractions of ferrite and retained austenite but a lower volume fraction of martensite. The measured phase fractions are consistent with the tensile data, *i.e.*, the QP-A sample shows a higher yield stress (Figure 1(b)) because of its high volume fraction of martensite (Figure 3(b)). The ferrite in the QP-A is formed only during the slow cooling from 900 °C to 690 °C, while the ferrite in the QP-I sample is formed during the intercritical annealing, as well as during the slow cooling from 780 °C to 690 °C (Figure 1(a)). Therefore, the QP-I sample shows a higher volume fraction of ferrite prior to the fast quenching from 690 °C to 250 °C, resulting in a higher volume fraction of ferrite in the final microstructure (Figure 3(b)). At 690 °C (Figure 1(a)), the QP-A sample has a higher volume fraction of austenite than the QP-I sample so that its carbon content in the austenite is lower. A lower carbon content in the austenite leads to a higher Ms temperature. As confirmed by the dilatometry curve shown in Figure 3(c), the Ms temperatures of QP-A and QP-I samples after austenization are 375 °C and 350 °C, respectively. In addition, large austenite grains in the QP-A sample, which can be deduced from the coarse M/A blocks, may contribute to higher Ms values. Therefore, after quenching from 690 °C to 250 °C (Figure 1(a)), the QP-A sample shows a higher volume fraction of martensite and a lower volume fraction of retained austenite (Figure 3(b)). As indicated by the straight dilatometry curve corresponding to the final quenching stage, no secondary martensite is formed in either the QP-A or QP-I sample. The partitioning step is designed for carbon partitioning from supersaturated martensite to austenite to improve the stability of austenite. Fresh martensite is reported to be very brittle. Consequently, the fraction of secondary martensite is better to be minimized or even completely avoided in Q&P steels for outstanding ductility–strength balance. In the current study, austenite grains are sufficiently stable to resist martensitic transformation during the final quenching. Both austenite grains in QP-A and QP-I samples exhibit great thermal stability due to the suitable partitioning conditions.

The Olson–Cohen model is employed to describe the mechanical stability of retained austenite during the tensile test,[7] which is expressed as

$$F_{\alpha'} = 1 - \exp\left[-\beta[1 - \exp(-\alpha\varepsilon)]^2\right], \qquad [1]$$

where $F_{\alpha'}$ is the transformation ratio of retained austenite to martensite at a true strain ε, and α and β are constants. α represents the nucleation rate of the shear bands, while β indicates the formation probability of a martensitic embryo. Both higher α and β values indicate faster kinetics of martensitic transformation during tensile test. The changes in the retained austenite fraction during the tensile tests for both samples on the interrupted tensile samples are shown in Figure 4(a). The best fitting of the Olson–Cohen model (Figure 4(b)) provides the α values in the QP-I and QP-A samples as 13.7 and 16.5,

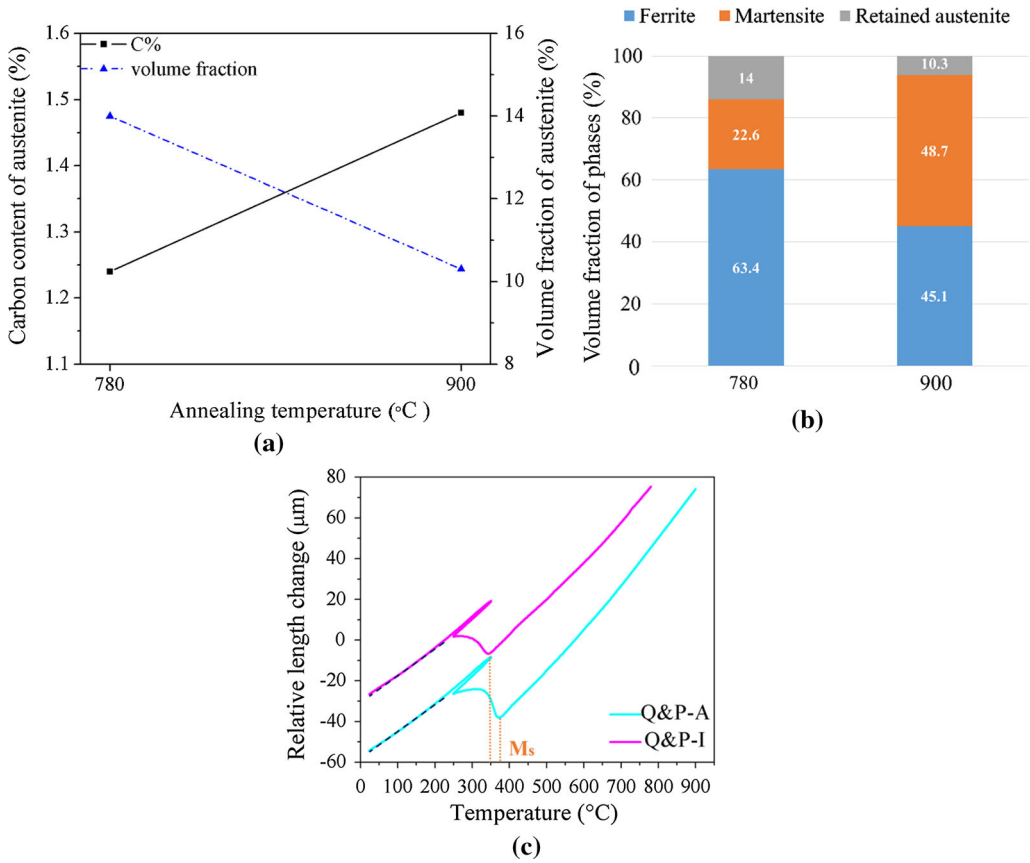

Fig. 3—(*a*) Volume fraction of retained austenite and its carbon content in the QP-I (780 °C) and QP-A (900 °C) samples; (*b*) volume fractions of ferrite, martensite, and austenite in the QP-I (780 °C) and QP-A (900 °C) samples; (*c*) relative length change as a function of temperature in the QP-I (780 °C) and QP-A (900 °C) samples during the Q&P treatment.

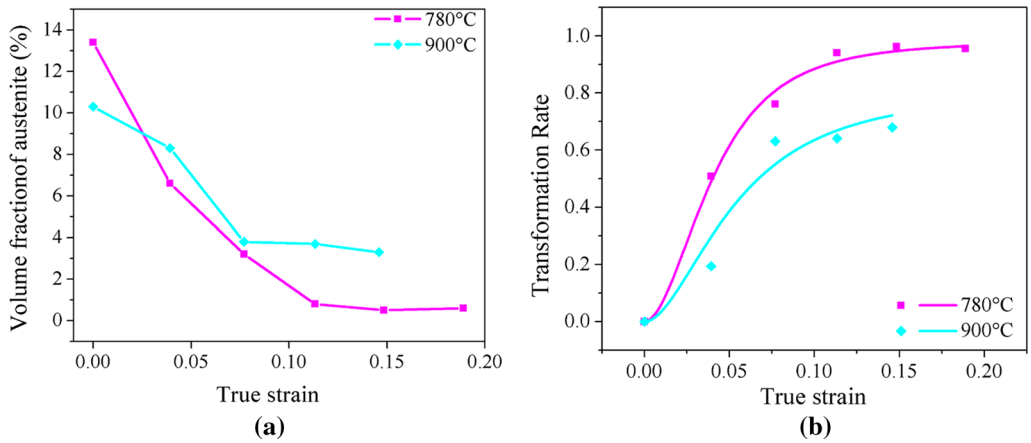

Fig. 4—(*a*) Evolution of retained austenite during tensile tests for the QP-I (780 °C) and QP-A (900 °C) samples, (*b*) transformation ratio of retained austenite during tensile tests for the QP-I (780 °C) and QP-A (900 °C) samples.

while β values are 3.9 and 1.5, respectively. QP-I and QP-A samples show different martensitic transformation kinetics during the tensile test (Figure 4(b)). Both samples show a gradual martensitic transformation at the beginning of plastic deformation. However, the martensitic transformation ceases at the true strain of 7.5 pct for the QP-A sample. Only ~ 70 pct of the retained austenite in the QP-A sample transforms to martensite up to fracture. By contrast, all retained austenite in the QP-A sample transforms gradually to martensite up to fracture (Figure 4(b)). Therefore, the QP-I sample does not

only have a higher volume fraction of retained austenite but also shows a more optimized mechanical stability of retained austenite.

The mechanical stability of retained austenite depends on various factors, including carbon content,[8] grain size,[9] morphology,[10] and dislocation density of retained austenite.[11] The effect of the carbon content on the lattice parameter of retained austenite in TRIP steel is more profound than the effects of Mn and Si.[12] Therefore, the carbon concentration x_c (in wt pct) of the retained austenite can be calculated from the lattice parameter of austenite obtained by the XRD measurements[13]:

$$a_\gamma = 0.3556 + 0.00453x_C, \quad [2]$$

where a_γ is the lattice parameter of the retained austenite. The carbon contents of the retained austenite in all samples as estimated by Eq. [2] are shown in Figure 3(a). It is understandable that a lower carbon content is observed in the retained austenite of the QP-I sample because it has a higher volume fraction of retained austenite. The carbon content in the QP-A sample is higher, indicating that its retained austenite has a higher mechanical stability, which explains why ~ 30 pct of retained austenite does not transform to martensite during the tensile test up to fracture (Figure 4(b)). In contrast, the carbon content in the retained austenite of the QP-I sample appears to be appropriate, resulting in a continuous martensitic transformation during the tensile tests (Figure 4(b)). In addition, the QP-I sample also has a higher volume fraction of retained austenite (Figure 4(a)). Therefore, the QP-I sample has a more pronounced TRIP effect than the QP-A sample, resulting in the higher work hardening rate. In addition to the more pronounced TRIP effect, the higher volume fraction of ferrite and the lower volume fraction of martensite in the QP-I sample may also contribute to its higher work hardening capability. In general, ferrite shows a higher dislocation multiplication rate than martensite such that a higher work hardening rate can be obtained in ferrite.

In summary, the current study demonstrates that the Q&P steel produced by intercritical annealing can achieve a similar ultimate tensile strength but a large uniform and total elongation compared to the steel produced by full austenization annealing. Comparison of the QP-I and QP-A samples shows that the QP-I sample exhibits a higher work hardening rate and a better tensile ductility. This finding is observed because the QP-I sample shows a more pronounced TRIP effect, as well as more ferrite and fewer martensite phases. For most of the existing industrial production lines with slow cooling rates, it is recommended to produce the Q&P steel for automotive lightweight applications by intercritical annealing instead of full austenization.

M.X. Huang acknowledges the financial support from Research Grants Council of Hong Kong (Grants Nos. HKU719712E, HKU712713E, 17203014).

REFERENCES

1. J.G. Speer, D.K. Matlock, B.C. De Cooman, and J.G. Schroth: *Acta Mater.*, 2003, vol. 51, pp. 2611–22.
2. M.J. Santofimia, L. Zhao, R. Petrov, C. Kwakernaak, W.G. Sloof, and J. Sietsma: *Acta Mater.*, 2011, vol. 59, pp. 6059–68.
3. E.J. Seo, L. Cho, Y. Estrin, and B.C. De Cooman: *Acta Mater.*, 2016, vol. 113, pp. 124–39.
4. H. Wendt and R. Wagner: *Acta Metall.*, 1982, vol. 30, pp. 1561–70.
5. E.P. Bagliani, M.J. Santofimia, L. Zhao, J. Sietsma, and E. Anelli: *Mater. Sci. Eng. A*, 2013, vol. 559, pp. 486–95.
6. G.H. Gao, H. Zhang, X.L. Gui, Z.L. Tan, and B.Z. Bai: *J. Mater. Sci. Technol.*, 2015, vol. 31, pp. 199–204.
7. Z.B. Dai, X. Wang, J.G. He, Z.G. Yang, C. Zhang, and H. Chen: *Metall. Mater. Trans. A*, 2017, vol. 48A, pp. 3168–74.
8. B.C. De Cooman, S.J. Lee, S. Shin, E.J. Seo, and J.G. Speer: *Metall. Mater. Trans. A*, 2016, vol. 48A, pp. 39–45.
9. X.C. Xiong, B. Chen, M.X. Huang, J.F. Wang, and L. Wang: *Scr. Mater.*, 2013, vol. 68, pp. 321–24.
10. H.S. Zhao, W. Li, L. Wang, S. Zhou, and X.J. Jin: *Metall. Mater. Trans. A*, 2016, vol. 47A, pp. 3943–55.
11. D. Walgraef and E.C. Aifantis: *Int. J. Eng. Sci.*, 1985, vol. 23, pp. 1365–72.
12. Z.H. Cai, H. Ding, R.D.K. Misra, and Z.Y. Ying: *Acta Mater.*, 2015, vol. 84, pp. 229–36.
13. E. Jimenez-Melero, N.H. Van Dijk, L. Zhao, J. Sietsma, S.E. Offerman, J.P. Wright, and S. Van der Zwaag: *Acta Mater.*, 2007, vol. 55, pp. 6713–23.